

Superconductivity in the presence of disorder in skutterudite-related $\text{La}_3\text{Co}_4\text{Sn}_{13}$ and $\text{La}_3\text{Ru}_4\text{Sn}_{13}$ compounds; electrical transport and magnetic studies

A. Ślebarski*, M. M. Maśka*, M. Fijałkowski*, C. A. McElroy†, and M. B. Maple†

**Institute of Physics, University of Silesia, 40-007 Katowice, Poland*

†*Department of Physics, University of California, San Diego, La Jolla, California 92093, USA*

$\text{La}_3\text{Co}_4\text{Sn}_{13}$ and $\text{La}_3\text{Ru}_4\text{Sn}_{13}$ were categorized as BCS superconductors. In a plot of the critical field H_{c2} vs T , $\text{La}_3\text{Ru}_4\text{Sn}_{13}$ displays a second superconducting phase at the higher critical temperature T_c^* , characteristic of inhomogeneous superconductors, while $\text{La}_3\text{Co}_4\text{Sn}_{13}$ shows bulk superconductivity below T_c . We observe a decrease in critical temperatures with external pressure and magnetic field for both compounds with $\frac{dT_c^*}{dP} > \frac{dT_c}{dP}$. The pressure dependences of T_c are interpreted according to the McMillan theory and understood to be a consequence of lattice stiffening. The investigation of the superconducting state of $\text{La}_3\text{Co}_x\text{Ru}_{4-x}\text{Sn}_{13}$ shows a T_c^* that is larger than T_c for $x < 4$. This unique and unexpected observation is discussed as a result of the local disorder and/or the effect of chemical pressure when Ru atoms are partially replaced by smaller Co atoms.

PACS numbers: 71.27.+a, 72.15.Qm, 71.30+h

I. INTRODUCTION

The effect of atomic disorder on the electronic properties of correlated electron systems, particularly those close to a quantum critical point (QCP)¹ has been a topic of active research. In the critical regime, the system is at the threshold of an instability and even weak perturbations, e.g., disorder can cause significant effects by changing the nature of the quantum macro state. In these disordered systems, a rather large residual resistivity $\rho_0 = \rho(T \rightarrow 0)$ is often encountered, even for single crystals, which means that even weak disorder is influential. As was argued theoretically², such a drastic influence is possible because the band width of a few eV and an effective Hubbard interaction U of the same order of magnitude result in a much more subtle energy balance that atomic disorder can disturb more easily. Therefore, investigations of atomic scale disorder in the form of defects and vacancies, granularity, and the effective increase in disorder by doping have received renewed attention in recent times particularly because of observations of novel phenomena in strongly correlated materials. The Kondo insulators are an example of thermoelectric materials where the defects lead to a high value of figure-of-merit $ZT = S^2\sigma T/(\kappa_e + \kappa_L)$, where S is the Seebeck coefficient, σ is the electrical conductivity, κ_e is the electronic thermal conductivity, and κ_L is the lattice contribution to the thermal conductivity³ due to the reduction of the lattice contribution to the thermal conductivity. The effect of disorder on superconducting properties has inspired a great deal of research, with the discovery of unconventional superconductivity in heavy fermion compounds⁴ and associated quantum critical behavior. In many superconductors, the critical temperature T_c decreases with increasing disorder and sufficiently strong disorder can, in fact, destroy superconductivity. As this disorder-driven transition from a superconducting to a non-superconducting ground state occurs, the localization effects become so

strong that often an insulating material results (at $T = 0$ this is known as a quantum phase transition). This transition is referred to as a superconductor-insulator transition⁵. There are known strongly correlated superconductors that show evidence of nanoscale disorder, meaning that the sample exhibits electronic inhomogeneity over the length scale of the coherence length. Such substantial nanoscale electronic disorder is characteristic of $\text{Bi}_2\text{Sr}_2\text{CaCu}_2\text{O}_{8+x}$ high- T_c materials, as well as $\text{PrOs}_4\text{Sb}_{12}$ ^{6,7}, CePt_3Si ^{8,9}, and CeIrIn_5 ¹⁰. Our recent investigation of the filled cage superconductors $\text{La}_3M_4\text{Sn}_{13}$ with $M = \text{Rh}$ ¹¹ and Ru ¹² have shown evidence of two superconducting phases: an inhomogeneous superconducting state below T_c^* and the superconducting phase at $T_c < T_c^*$. This anomaly was interpreted in the context of the presence of an inhomogeneous superconducting phase between T_c and T_c^* . In this work, we present a comprehensive thermodynamic and high-pressure electrical resistivity study on $\text{La}_3\text{Co}_x\text{Ru}_{4-x}\text{Sn}_{13}$ to explain the superconductivity in the presence of disorder. $\text{La}_3\text{Co}_4\text{Sn}_{13}$ clearly exhibits a homogeneous superconducting phase at T_c , while in contrast $\text{La}_3\text{Ru}_4\text{Sn}_{13}$ and its Co-alloys show evidence of nanoscale inhomogeneity with the presence of T_c^* . The impact of disorder on the ground state of superconducting materials has played an important role in condensed matter physics over the years. We believe that our results contribute towards developing a broader understanding of the complex behavior in novel superconducting strongly correlated electron systems.

II. EXPERIMENTAL DETAILS

Polycrystalline $\text{La}_3\text{Co}_4\text{Sn}_{13}$ and $\text{La}_3\text{Ru}_4\text{Sn}_{13}$ samples were prepared by arc melting the constituent elements on a water cooled copper hearth in a high-purity argon atmosphere with an Al getter. The dilute $\text{La}_3\text{Co}_x\text{Ru}_{4-x}\text{Sn}_{13}$ alloys were prepared by diluting nominal compositions of the parent compounds. The samples

were then annealed at 870 °C for 2 weeks. All samples were carefully examined by x-ray diffraction analysis and found to have a cubic structure (space group $Pm\bar{3}n$)¹³ and for $x = 1$ and 3.5, the samples were single phase while for $x = 2$ and 3, the alloys were a mixture of two phases.

Stoichiometry and homogeneity were verified by the microprobe technique (scanning microscope JSM-5410) and by XPS analysis. As an example, measurements of $\text{La}_3\text{Co}_4\text{Sn}_{13}$ showed a composition close to the nominal ratio 3:4:13 (i.e., 14.87:19.93:65.20 for La:Co:Sn). For the $\text{La}_3\text{Ru}_4\text{Sn}_{13}$ and $\text{La}_3\text{Co}_x\text{Ru}_{4-x}\text{Sn}_{13}$ alloys, the composition of the samples were also close to the nominal ratio 3:4:13 stoichiometry, and in Table I, we present the results from measurements of $\text{La}_3\text{Ru}_3\text{CoSn}_{13}$ noted at different points of the surface.

Ambient pressure electrical resistivity ρ was investigated by a conventional four-point ac technique using a Quantum Design Physical Properties Measurement System (PPMS). Electrical resistivity measurements under pressure were performed in a beryllium-copper, piston-cylinder clamped cell. A 1:1 mixture of *n*-pentane and isoamyl alcohol in a teflon capsule served as the pressure transmitting medium to ensure hydrostatic conditions during pressurization at room temperature. The local pressure in the sample chamber was inferred from the inductively determined, pressure-dependent superconducting critical temperature of a Sn ingot¹⁴.

Specific heat C was measured in the temperature range 0.4 – 300 K and in external magnetic fields up to 9 T using a Quantum Design PPMS platform. The dc magnetization M and magnetic susceptibility χ results were obtained using a commercial (Quantum Design) superconducting quantum interference device magnetometer from 1.8 K to 300 K in magnetic fields up to 7 T.

III. RESULTS AND DISCUSSION

A. Electric transport, magnetic properties, and specific heat of $\text{La}_3\text{Co}_x\text{Ru}_{4-x}\text{Sn}_{13}$ near the critical temperature T_c or T_c^*

We performed a comprehensive thermodynamic and electrical resistivity study which reveal a homogeneous superconducting phase for $\text{La}_3\text{Co}_4\text{Sn}_{13}$, whereas for $\text{La}_3\text{Ru}_4\text{Sn}_{13}$ and the Co-substituted $\text{La}_3\text{CoRu}_3\text{Sn}_{13}$ samples there is evidence of two superconducting phases. Fig. 1 shows results of resistivity measurements of $\text{La}_3\text{Ru}_3\text{CoSn}_{13}$ vs temperature T in various magnetic fields up to 5.2 T. Here we define the critical temperature at 50 % of the normal state resistivity value. Similar $\rho(T)$ dependencies vs B were presented for $\text{La}_3\text{Co}_4\text{Sn}_{13}$ and $\text{La}_3\text{Ru}_4\text{Sn}_{13}$ very recently (c.f. Refs. 11 and 12). In Fig. 2, we show the $H - T$ phase diagram obtained for several investigated compounds and alloys of the system $\text{La}_3\text{Co}_x\text{Ru}_{4-x}\text{Sn}_{13}$, where T_c is obtained

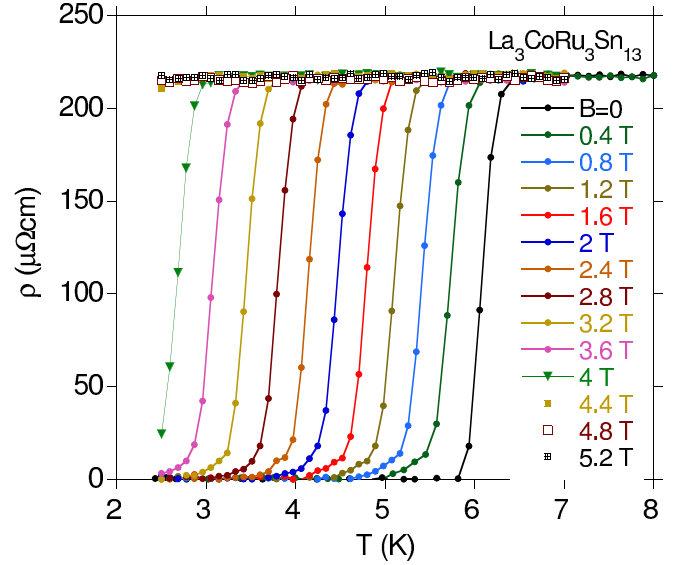


FIG. 1. The temperature dependence of the resistivity ρ of $\text{La}_3\text{CoRu}_3\text{Sn}_{13}$ at various externally applied magnetic fields, demonstrating the smooth suppression of T_c^* .

from electrical resistivity under increasing magnetic fields (curves: *a* for $\text{La}_3\text{CoRu}_3\text{Sn}_{13}$, *d* for $\text{La}_3\text{Ru}_4\text{Sn}_{13}$, and *g* for $\text{La}_3\text{Co}_4\text{Sn}_{13}$).

The Ginzburg-Landau (GL) theory fits the data well and is shown in the $H - T$ plots in Fig. 2. The best fit of the equation $H_{c2}(T) = H_{c2}(0) \frac{1-t^2}{1+t^2}$, where $t = T/T_c$ gives the value of the upper critical field $H_{c2}(0)$ presented in Table II. Within the weak-coupling theory¹⁵ the upper critical field through the relation $\mu_0 H_{c2}(0) = \Phi_0 / 2\pi \xi_0^2$ can be used to estimate the coherence length (where the flux quantum $\Phi_0 = h/2e = 2.068 \times 10^{-15} \text{ Tm}^2$), and these values are also listed in Table II. The table also displays the $H_{c2}(0) = 0.693 T_c \frac{dH_{c2}}{dT} \big|_{T=T_c}$ ^{16,17} based on the results presented in Fig. 2.

Shown in Fig. 3 is the specific heat C plotted as C vs T at various magnetic fields (in panel *a*), and ac and dc magnetic susceptibility (panel *b*) for $\text{La}_3\text{Co}_{3.5}\text{Ru}_{0.5}\text{Sn}_{13}$. The heat capacity data for $\text{La}_3\text{Co}_4\text{Sn}_{13}$ (not shown in Fig. 3, c.f. Ref. 11) indicates bulk superconductivity below $T_c = 1.95 \text{ K}$ in agreement with resistivity data, while $\text{La}_3\text{Co}_{3.5}\text{Ru}_{0.5}\text{Sn}_{13}$ shows a broad transition to the superconducting state with the same T_c from the resistivity and susceptibility data.

For $\text{La}_3\text{CoRu}_3\text{Sn}_{13}$, the superconductivity shown in C/T data (in Fig. 4a and Fig. 5) also shows broad transition with the maximum in $\Delta C/T$ at $T_c \approx 5 \text{ K}$ spanning the maximum in χ'' in Fig. 4b. Under certain conditions, the ac losses in superconducting transition can exceed those of a normal metal, leading to a peak in χ'' vs T ¹⁸. However, it was argued that a χ'' maximum can occur in surface superconductors at sufficiently low frequencies, this is not the case in the ac magnetic susceptibility shown in Fig. 3¹⁹. The perfect diamagnetism of the full Meissner state $\chi' = -1/(4\pi d) = 9.55 \times 10^{-3}$

TABLE I. Atomic % reflecting the stoichiometric ratios for $\text{La}_3\text{Ru}_3\text{CoSn}_{13}$ sample at different areas on the surface.

element	stoichiometry in at. %				
	assumed		measured		
La	15	15.94	15.55	17.07	14.16
Ru	15	13.97	12.45	12.75	13.70
Co	5	4.72	6.62	3.62	5.07
Sn	65	65.37	65.38	66.47	67.07

TABLE II. Superconducting state quantities for $\text{La}_3\text{Co}_x\text{Ru}_{4-x}\text{Sn}_{13}$ near the bulk superconducting phase T_c or the inhomogeneous phase below T_c^* .

$\text{La}_3\text{Co}_x\text{Ru}_{4-x}\text{Sn}_{13}$	$x = 4$	$x = 3.5$	$x = 1$	$x = 0$
T_c (K)	1.95	2.41	≈ 5	1.58
T_c^* (K)			5.58	3.76
$\frac{dH_{c2}}{dT} _{T=T_c}$ (T/K)	-0.904	-1.34	-1.3 ($T \rightarrow T_c^*$)	-1.33 ($T \rightarrow T_c$), -1 ($T \rightarrow T_c^*$)
$H_{c2}(0) = 0.693T_c \frac{dH_{c2}}{dT} _{T=T_c}$ (T)	1.22	2.24	4.97 ($T \rightarrow T_c^*$)	1.45 ($T \rightarrow T_c$), 2.61 ($T \rightarrow T_c^*$)
$H_{c2}(0)$ (T)	1.38	3.05	5.28	1.34 ($T_c = 0$), 3.08 ($T_c^* = 0$)
$\xi(0)$ (nm)	16	11	$\xi^*(0) = 8$	18, $\xi^*(0) = 9$
$\frac{\Delta C}{\gamma T_c}$	1.5(5)	1.7	undefined	1.6(1)
$\frac{dT_c}{dP}$ (K/GPa)	0.05	-0.12		-0.03
$\frac{dT_c^*}{dP}$ (K/GPa)			-0.32	-0.24

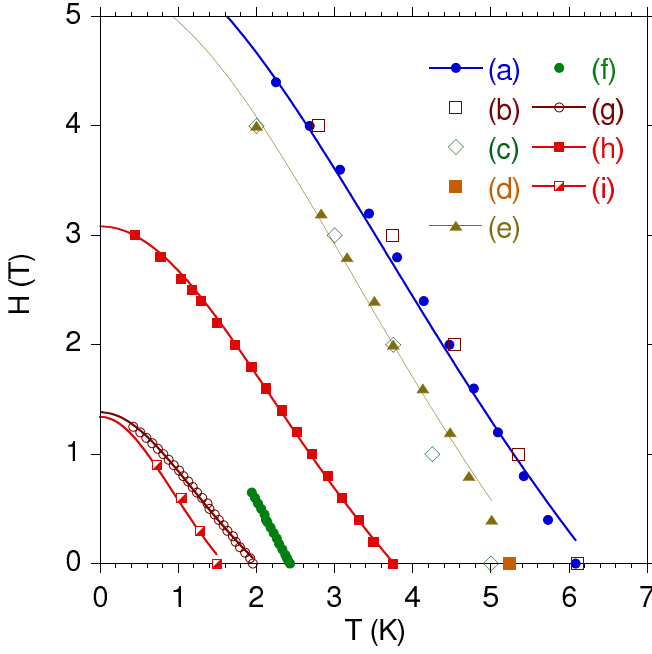


FIG. 2. Temperature dependence of the upper critical fields H_{c2} in the $H - T$ diagram for $\text{La}_3\text{Co}_x\text{Ru}_{4-x}\text{Sn}_{13}$. The solid lines represent a Ginzburg-Landau fitting model for $H_{c2}(T)$. $\text{La}_3\text{CoRu}_3\text{Sn}_{13}$: Points a represent T_{cs} obtained from resistivity under H at 50% decrease of the normal state ρ -value. Points b show the temperatures where anomalous behavior begins in $\Delta C/T$ at the high-temperature side of the specific heat peak. Points c are attributed to temperature of the maxima in the best fits of $f(\Delta)$ to the experimental data $\Delta C(T)/T$, d is the temperature of maximum in $\chi''(T)$ at the magnetic field $B = 0$, while e show the temperatures where $\rho(T) \rightarrow 0$ (c.f. Fig. 1). $\text{La}_3\text{Ru}_4\text{Sn}_{13}$: points h represent T_c^* obtained from the ρ -data, while i are T_{cs} from the specific heat data (Ref. 12. $\text{La}_3\text{Co}_4\text{Sn}_{13}$: g are T_{cs} from $\rho(T)$ at 50% decrease of the normal state ρ -value (Ref. 11. f are T_{cs} obtained from $C(T)$ vs B for $\text{La}_3\text{Co}_{3.5}\text{Ru}_{0.5}\text{Sn}_{13}$ (c.f. Fig. 3).

emu/g for mass density $d = 8.3 \text{ g/cm}^3$ (Refs. 27 and 28) is reached below the temperature of the maximum in χ'' , it should also be noted that χ'' depends on the frequency of the magnetic field, and that is characteristic of magnetically inhomogeneous materials. We believe that the superconductivity in $\text{La}_3\text{CoRu}_3\text{Sn}_{13}$ is completely inhomogeneous superconductivity to explain the anomalies in the specific heat and χ'' . Namely, we believe that the resistivity drop marks the onset of an inhomogeneous superconducting phase with spatial distribution of the magnitude of the superconducting gap, as a bulk property of the sample. Since the drop of the resistivity at T_c^* is not accompanied by a change of χ'' , the volume occupied by the inhomogeneous phase is too small to cancel out normal-state paramagnetic contributions. On the other hand, the superconducting regions must be arranged as to form the necessary continuous paths reflected in the resistivity measurements.

Following Ref. 29 we assume a simple Gaussian gap

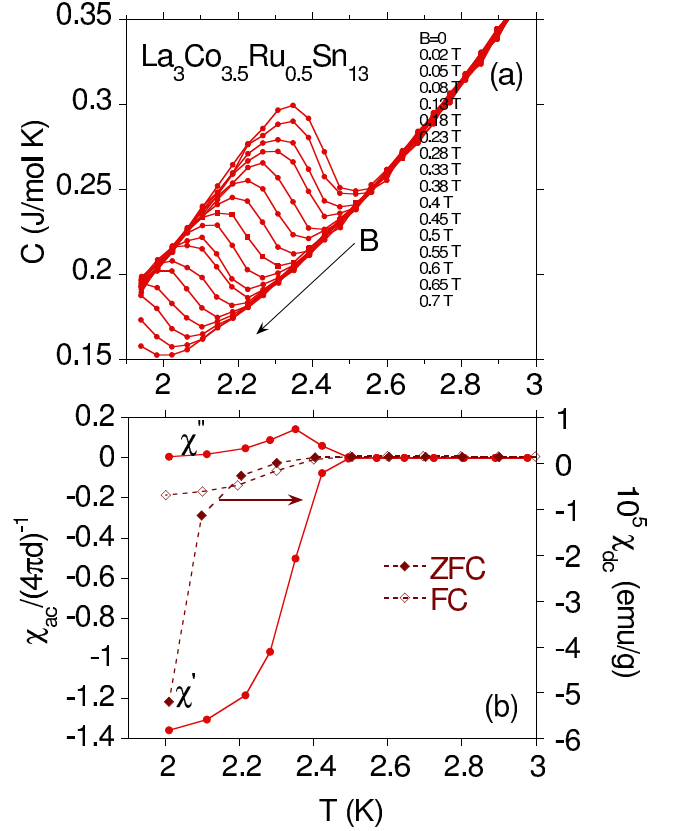


FIG. 3. (a) The temperature dependence of the specific heat $C(T)$ of $\text{La}_3\text{Co}_{3.5}\text{Ru}_{0.5}\text{Sn}_{13}$ at different magnetic fields B . (b) The ac magnetic susceptibility χ_{ac} at $B = 12 \text{ Gs}$ divided by theoretical value of the full Meissner state $\chi' = 1/(4\pi d)$, and zero-field-cooled (ZFC) and field-cooled (FC) dc magnetic susceptibility in an applied field of $B = 500 \text{ Gs}$.

distribution

$$f(\Delta) \propto \exp \left[-\frac{(\Delta - \Delta_0)^2}{2d} \right], \quad (1)$$

where Δ_0 and d are treated as fitting parameters. The best fit of $f(\Delta)$ to the experimental data $\Delta C(T)/T$ gives the points c in Fig. 2, in good agreement with the points e in Fig. 2. Points d represents the temperature of the maximum in χ'' . The behavior observed in this strongly disordered alloy is qualitatively different than that in $\text{La}_3\text{Ru}_4\text{Sn}_{13}$ ¹², or $\text{La}_3\text{Rh}_4\text{Sn}_{13}$ ¹¹ with clear evidence for two superconducting phases: the *high temperature* inhomogeneous superconducting state below T_c^* and the second (bulk) superconducting phase below T_c , where $T_c^* > T_c$. We also note that the $C(T)/T$ data for $\text{La}_3\text{CoRu}_3\text{Sn}_{13}$ is not well approximated by $C(T)/T \sim \exp(-\Delta(0)/k_B T)$, while the bulk superconducting phases in both $\text{La}_3\text{Ru}_4\text{Sn}_{13}$ and $\text{La}_3\text{Co}_4\text{Sn}_{13}$ are well fit by this expression (c.f., Fig. 5). Excluding the case of $\text{La}_3\text{CoRu}_3\text{Sn}_{13}$, we found $C(T)$ follows the behavior described by the BCS theory in the weak-coupling limit, which indicates *s*-wave superconductivity. The

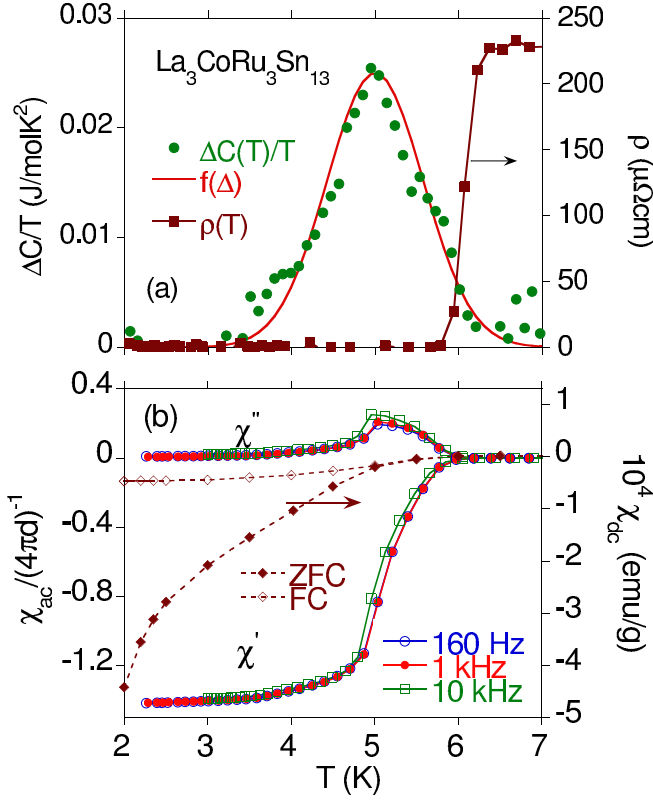


FIG. 4. (a) The temperature dependence of the specific heat $\Delta C(T)/T$ with a Gaussian gap distribution fit $f(\Delta)$ and resistivity $\rho(T)$, both at $B=0$ for $\text{La}_3\text{CoRu}_3\text{Sn}_{13}$. For the sample under $B=0$, $\Delta C(T)/T = C(T, B=0)/T - C(T, B=5T)/T$, see Fig. 5. (b) The ac magnetic susceptibility ($B=12$ Gs) χ' and χ'' at different frequencies, and ZFC and FC dc magnetic susceptibility ($B=500$ Gs).

BCS theory for s -wave superconductors provides a relation $\Delta C/(\gamma T_c) = 1.43$ between the jump of the specific heat ΔC at the critical temperature T_c and the normal metallic state contribution γ ; the theoretical value $\Delta C/(\gamma T_c) = 1.43$ is very close to the values presented in Table II.

In Fig. 6, we show that the hysteresis loop in the superconducting state of $\text{La}_3\text{CoRu}_3\text{Sn}_{13}$ is about 3 K, while in the case of the remaining compounds, it is nearly an order of magnitude smaller. The broad hysteresis loop suggests strongly inhomogeneous material.

We expect that external pressure applied to strongly disordered materials should drive lattice instabilities from the compounds by varying the dominant parameters of the superconducting state, e.g., electronic density of states at the Fermi level. Most of the known superconductors show a decrease of T_c with increasing applied pressure³⁰; however, increasing pressure should also partially mitigate the inhomogeneity and stabilize the structural properties of the disordered system, and as a consequence, T_c^* is also expected to decrease with pressure. The evidence of this is shown in Figs. 7 - 9 and summarized in Fig. 10. The observed increase of T_c

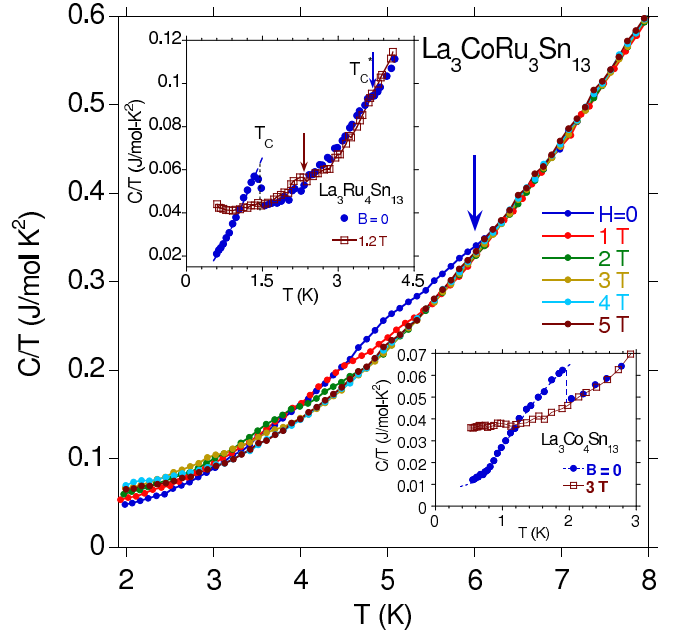


FIG. 5. The specific heat $\Delta C(T)/T$ under various magnetic fields for $\text{La}_3\text{CoRu}_3\text{Sn}_{13}$. The arrow indicates the beginning of the superconductivity at $B=0$, the transitions under magnetic fields $B \neq 0$ are similarly broad. The insets display the C/T data near T_c for $\text{La}_3\text{Ru}_4\text{Sn}_{13}$ and $\text{La}_3\text{Co}_4\text{Sn}_{13}$. In case of $\text{La}_3\text{Ru}_4\text{Sn}_{13}$ the bulk effect at T_c and inhomogeneous superconducting phase between T_c^* and T_c are both shown. The dotted line is the best fit to the data for the expression $C(T)/T = \gamma + \beta T^2 + A \exp(-\Delta(0)/k_B T)$.

with pressure shown in Fig. 10 for $\text{La}_3\text{Co}_4\text{Sn}_{13}$ was recently discussed as a possible result of a subtle structural distortion below $T = 140$ K¹¹.

The pressure coefficients $\frac{dT_c}{dP}$ and $\frac{dT_c^*}{dP}$ obtained from the respective T_c vs P data shown in Fig. 10 are listed in Table II. The pressure coefficients of T_c^* are almost twice large as those of T_c , while for $\text{La}_3\text{Co}_4\text{Sn}_{13}$, the $\frac{dT_c}{dP} = 0.05$ K/GPa is positive. The P -dependence of T_c has been discussed according to the Eliashberg theory of strong-coupling superconductivity³¹. We employ the McMillan expression^{32,33}

$$T_c = \frac{\theta_D}{1.45} \exp \left\{ \frac{-1.04(1 + \lambda)}{\lambda - \mu^*(1 + 0.62\lambda)} \right\}, \quad (2)$$

which is a solution of the finite-temperature Eliashberg equations, to connect the value of T_c with the electron-phonon coupling parameter λ , Debye temperature θ_D and the Coulomb repulsion μ^* (the value of μ^* was chosen to be 0.1 as is typical for s and p band superconductors). This yields $\lambda \approx 0.4$ for T_c s and a larger λ value ~ 0.5 for T_c^* s. However, in the both superconducting states, relatively small λ negates the strong coupling superconductivity. The coupling λ is given by

$$\lambda = \frac{N(E_F)\langle I^2 \rangle}{M\langle \omega^2 \rangle}, \quad (3)$$

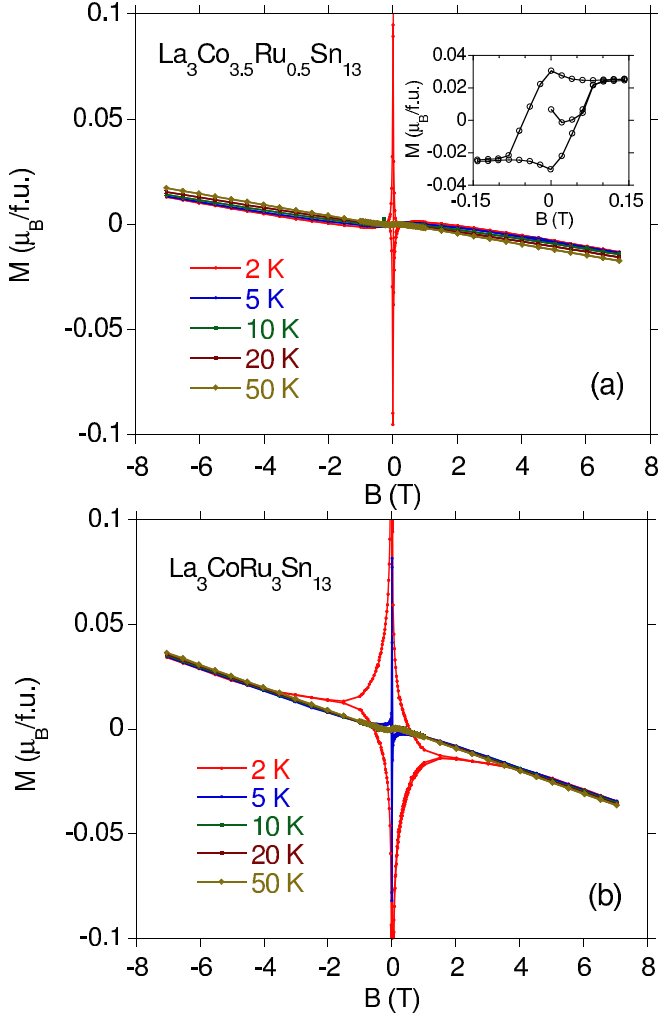


FIG. 6. Magnetization M per formula unit vs magnetic field at various temperatures. The inset shows a symmetric hysteresis loop at $T = 1.8$ K for the superconducting state in $\text{La}_3\text{Co}_4\text{Sn}_{13}$. Panel (a) shows the data for $\text{La}_3\text{Co}_{3.5}\text{Ru}_{0.5}\text{Sn}_{13}$, panel (b) displays M for $\text{La}_3\text{CoRu}_3\text{Sn}_{13}$.

where $\langle I^2 \rangle$ is the square of the electronic matrix element of electron-phonon interactions averaged over the Fermi surface, $\langle \omega^2 \rangle$ is an average of the square of the phonon frequency, and M is the atomic mass. Usually, μ^* and $\langle I^2 \rangle$ are very weakly pressure dependent, so that the main pressure effect on the transition temperature comes from θ_D and $N(E_F)$ ($\langle \omega^2 \rangle$ depends on θ_D). The pressure dependence of θ_D is given by the Grüneisen parameter $\gamma_G = -\frac{d\ln\theta_D}{d\ln V}$, which represents the lattice stiffening. Using the McMillan expression it was found³⁴ that γ_G strongly determines the magnitude and sign of $\frac{dT_c}{dP}$. Our data suggest a larger γ_G for the inhomogeneous superconducting state with respect to the bulk effect observed below T_c ; in case of $\text{La}_3\text{Co}_4\text{Sn}_{13}$, the Grüneisen parameter is expected to be smaller. It is also possible that in the case of inhomogeneous superconductivity, the pressure dependence of the density of states at the Fermi

level is more pronounced than in bulk superconductors, and may lead to a larger value of $\frac{dT_c^*}{dP}$ than $\frac{dT_c}{dP}$.

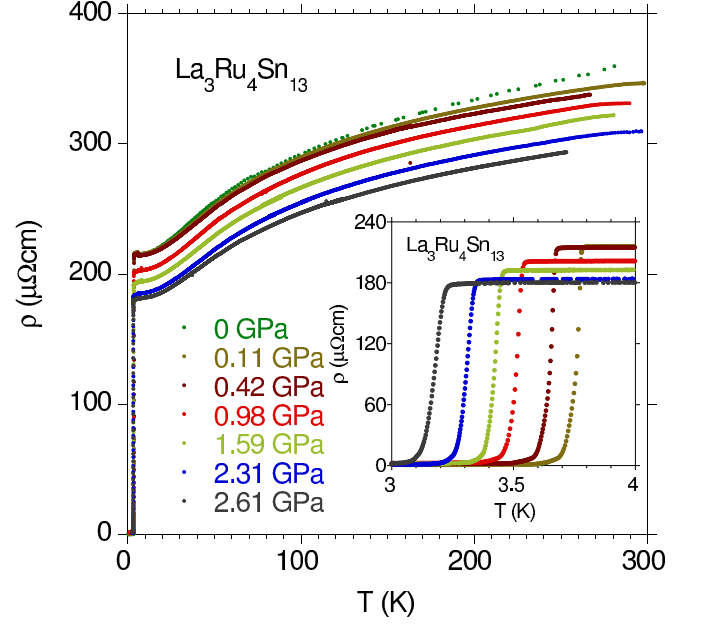


FIG. 7. Electrical resistivity ρ of $\text{La}_3\text{Ru}_4\text{Sn}_{13}$ at various applied pressures. The inset displays the low temperature details, showing the smooth suppression of T_c .

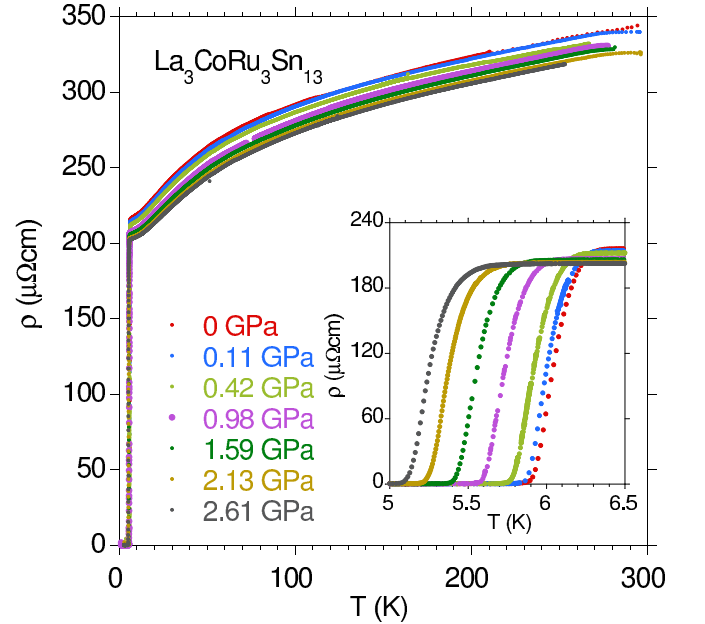


FIG. 8. Resistivity of $\text{La}_3\text{CoRu}_3\text{Sn}_{13}$ at different applied pressure. The inset displays the details.

Since the Co radius is smaller than that of Ru, increasing the amount of Co in the $\text{La}_3\text{Co}_x\text{Ru}_{4-x}\text{Sn}_{13}$ system leads to an effectively negative internal pressure. With x increasing from 0 to 1, T_c increases as well, but further, for x going from 1 to 4, T_c decreases almost linearly from

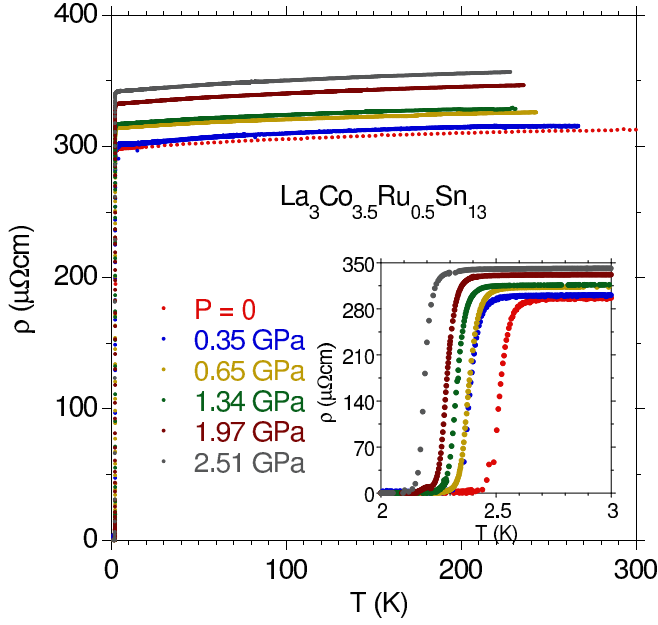


FIG. 9. Resistivity of $\text{La}_3\text{Co}_{3.5}\text{Ru}_{0.5}\text{Sn}_{13}$ at different applied pressure. The inset displays the details.

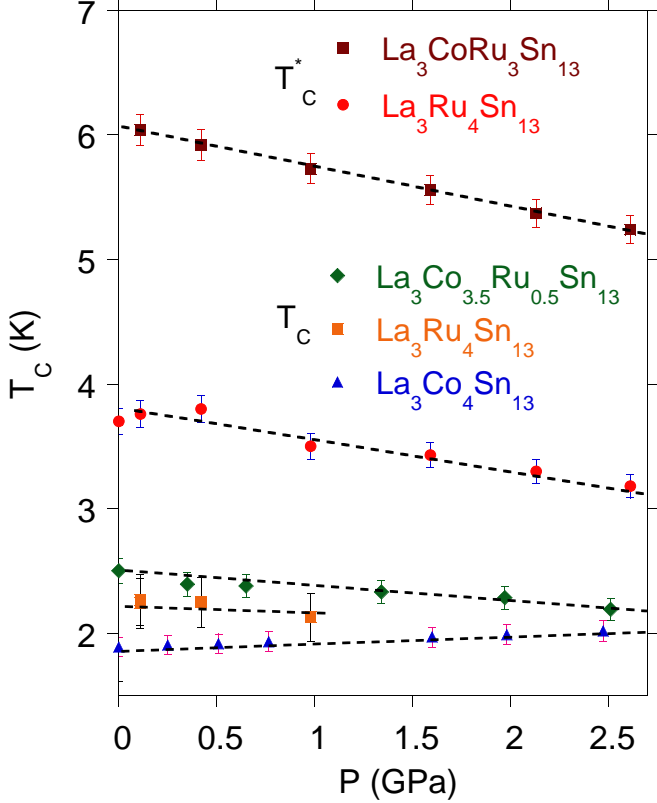


FIG. 10. Critical temperatures T_c and T_c^* vs pressure P . The critical temperatures are obtained from resistivity under applied pressure at 50% of the normal state value. For $\text{La}_3\text{Ru}_4\text{Sn}_{13}$, T_c is estimated as a very weak change in $\rho(T)$ below T_c^* .

5 K to 1.95 K (see Fig. 11). The dependence of T_c^* on the chemical pressure is consistent with the effects of external pressure. With x increasing from 0 to 1, T_c^* increases from about 3.76 K to 5.58 K, and can be interpreted as a continuation of the dependence on the external pressure for $P < 0$. In this case, however, T_c^* is slightly less sensitive to the chemical pressure than T_c .

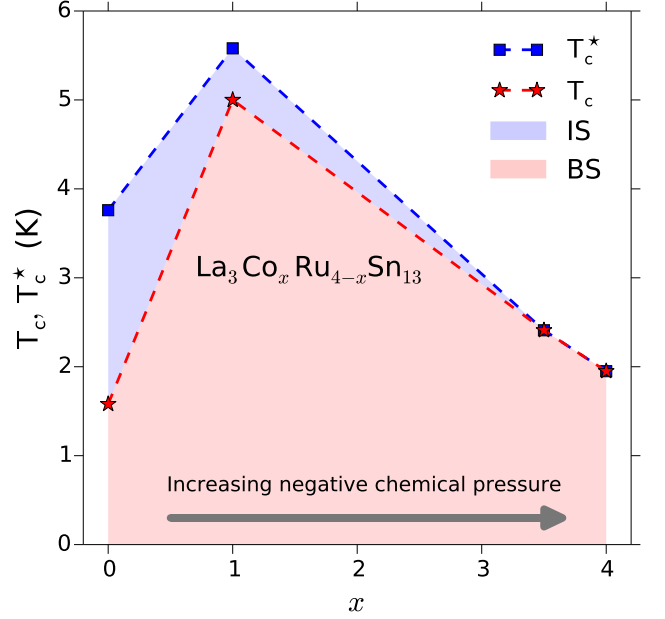


FIG. 11. Ambient pressure T_c and T_c^* as a function of x for $\text{La}_3\text{Co}_x\text{Ru}_{4-x}\text{Sn}_{13}$. Dashed lines are a guide to the eye. The blue area represents the inhomogeneous superconducting phase (IS), whereas the red area represents bulk superconductivity (BS).

It is difficult to understand the abnormally large critical temperature for $\text{La}_3\text{CoRu}_3\text{Sn}_{13}$, that is much larger than the T_c^* characterizing the inhomogeneous superconducting phase in of $\text{La}_3\text{Ru}_4\text{Sn}_{13}$. Typically, disorder strongly reduces the critical temperature due to the elevated impurity scattering; therefore, large value of T_c^* is surprising. It is, however, also possible to enhance superconductivity by local disorder³⁵. In this case, the superconductor may be inhomogeneous with lower and higher T_c regions. Above T_c^* , superconducting clusters appear, which at T_c^* form a network of continuous paths through the entire sample. The random character of the Co substitution leads to a statistical (chaotic) distribution of these clusters. Despite the drop in the electrical resistivity, the fraction of the volume occupied by the superconducting state can still be small. This is a typical percolation scenario³⁶. At a lower temperature T_c , the previously normal regions become superconducting and a macroscopic (bulk) superconducting state is formed. This is the transition that is seen in the specific heat and susceptibility measurements.

IV. CONCLUDING REMARKS

In most of the known superconductors, the transition temperature T_c decreases as a consequence of increased disorder. However, there are known examples of strongly correlated superconductors which show evidence of nanoscale disorder leading to an inhomogeneous superconducting state and, as a consequence, the critical temperature $T_c^* > T_c$. Both superconducting phases: the T_c -bulk phase and the T_c^* *high-temperature* inhomogeneous phase whose onset is observed between T_c^* and T_c are present in the skutterudite-related $\text{La}_3\text{Rh}_4\text{Sn}_{13}$ and $\text{La}_3\text{Ru}_4\text{Sn}_{13}$ compounds. In these compounds, we observed a decrease of the critical temperature with the application of external pressure, however, the pressure coefficients $\frac{dT_c^*}{dP}$ are nearly twice as large as their respective $\frac{dT_c}{dP}$ values. In the case of $\text{La}_3\text{Co}_4\text{Sn}_{13}$, $\frac{dT_c}{dP}$ is positive. The P -variations of T_c were interpreted in the context of the Eliashberg theory and discussed as a consequence of the lattice stiffening. The results shown in this work should be of interest for understanding the x -dependent superconducting state of $\text{La}_3\text{Co}_x\text{Ru}_{4-x}\text{Sn}_{13}$ where T_c^* is larger than T_c for $\text{La}_3\text{Ru}_4\text{Sn}_{13}$, (e.g., for $\text{La}_3\text{CoRu}_3\text{Sn}_{13}$

it is almost twice as large). This unique observation is not predicted by the BCS theory and not observed in other chemically substituted superconductors. We suggest that local disorder is responsible for the increase in T_c in strongly inhomogeneous regions in the sample and/or the effect of chemical pressure when $\text{La}_3\text{Ru}_4\text{Sn}_{13}$ is substituted with by Co. This scenario should be verified theoretically.

V. ACKNOWLEDGMENTS

The research was supported by National Science Centre (NCN) on the basis of Decision No. DEC-2012/07/B/ST3/03027. M.M.M. acknowledges support by NCN under grant DEC-2013/11/B/ST3/00824. High-pressure research at the University of California, San Diego, was supported by the National Nuclear Security Administration under the Stewardship Science Academic Alliance program through the U. S. Department of Energy under Grant Number de-na0001841. One of us (A.Ś.) is grateful for the hospitality at the University of California, San Diego (UCSD).

-
- ¹ Cf. special issue of J. Phys. Condensed Matter. **8**, No. 48 (1996) (eds. P. Coleman, M. B. Maple, and A. Millis).
 - ² J. Spalek and W. Wójcik, Acta Phys. Polon. B **34**, 399 (2003).
 - ³ Y. Zhang, M. S. Dresselhaus, Y. Shi, Z. Ren, and G. Chen, Nano Lett. **11**, 1166 (2011).
 - ⁴ F. Steglich, J. Aarts, C. D. Bredl, W. Lieke, D. Meschede, W. Franz, and H. Schäfer, Phys. Rev. Lett. **43**, 1892 (1979).
 - ⁵ A. M. Goldman and N. Marković, Physics Today, **51** 39 (1998).
 - ⁶ M. B. Maple, P.-C. Ho, V. S. Zapf, N. A. Frederick, E. D. Bauer, W. M. Yuhasz, F. M. Woodward and J. W. Lynn, J. Phys. Soc. Jpn. Suppl. **71**, 23 (2002)
 - ⁷ R. Vollmer, A. Falt, C. Pfleiderer, H. v. Löhneysen, E. D. Bauer, P.-C. Ho, V. Zapf, and M. B. Maple, Phys. Rev. Lett. **90**, 057001 (2003).
 - ⁸ J. S. Kim, D. J. Mixson, D. J. Burnette, T. Jones, P. Kumar, B. Andraka, G. R. Stewart, V. Craciun, W. Acree, H. Q. Yuan, D. Vandervelde, and M. B. Salamon, Phys. Rev. B **71**, 212505 (2005)
 - ⁹ T. Takeuchi, T. Yasuda, M. Tsujino, H. Shishido, R. Settai, H. Harima, and Y. Onuki, J. Phys. Soc. Jpn. **76** 014702 (2007).
 - ¹⁰ A. Bianchi, R. Movshovich, M. Jaime, J. D. Thompson, P. G. Pagliuso, and J. L. Sarrao, Phys. Rev. B **64**, 220504(R) (2001).
 - ¹¹ A. Ślebarski, M. Fijałkowski, M. M. Maška, M. Mierzejewski, B. D. White, and M. B. Maple, Phys. Rev. B, **70**, 144516 (2014).
 - ¹² A. Ślebarski, M. Fijałkowski, J. Goraus, L. Kalinowski, and P. Witas, J. Alloys Compd, **615**, 921 (2014).
 - ¹³ J. P. Remeika, G.P. Espinosa, A. S. Cooper, H. Barz, J.M. Rowel, D. B. McWhan, J. M. Vandenberg, D. E. Moncton, Z. Fizk, L. D. Woolf, H. C. Hamaker, M. B. Maple, G. Shirane, and W. Thomlinson, Sol. State Commun. **34**, 923 (1980); J. L. Hodeau, M. Marezio, J. P. Remeika, and C. H. Chen, *ibid.* **42**, 97 (1982).
 - ¹⁴ T. F. Smith, C. W. Chu, and M. B. Maple, Cryogenics **9**, 54 (1969).
 - ¹⁵ V. V. Schmidt, *The Physics of Superconductors*, ed. P. Müller and A. V. Ustinov (Berlin: Springer, 1977).
 - ¹⁶ N. R. Werthamer, E. Helfand, and P. C. Hohenberg, Phys. Rev. **147**, 295 (1966).
 - ¹⁷ E. Helfand N. R. Werthamer, Phys. Rev. **147**, 288 (1966).
 - ¹⁸ M. Strongin and E. Maxwell, Phys. Lett. **6**, 49 (1963).
 - ¹⁹ A surface superconductivity effect can be observed above the bulk critical field H_{c2} for type II superconductors. Saint-James and de Gennes²⁰ have shown theoretically that a surface superconducting layer with a critical field $H_{c3} = 1.69H_{c2}$ can exist above H_{c2} but only when the external magnetic field is parallel to the sample surface. Experimental evidence²¹⁻²⁶ has confirmed the existence of the surface critical field H_{c3} . In case of $\text{La}_3\text{Ru}_4\text{Sn}_{13}$ the hypothetical $H_{c3}/H_{c2} = 1.8$ ratio is closed to the calculated one, however, $T_c \neq T_c^*$ behavior observed for the surface and bulk superconductivity is not theoretically expected. Moreover, the *high- T_c* superconducting state is observed under the zero magnetic field. The both arguments seem exclude the surface superconductivity effect in $\text{La}_3\text{Ru}_4\text{Sn}_{13}$ and $\text{La}_3\text{CoRu}_3\text{Sn}_{13}$.
 - ²⁰ D. Saint-James and P. D. Gennes, Phys. Lett. **7**, 306 (1964).
 - ²¹ C. F. Hempstead and Y. B. Kim, Phys. Rev. Lett. **12**, 145 (1964).
 - ²² W. J. Tomasch and A. S. Joseph, Phys. Rev. Lett. **12**, 148 (1964).

- ²³ S. Gygax, J. L. Olsen, and R. H. Kroppschot, Phys. Lett. **8**, 228 (1964).
- ²⁴ M. Cardona and B. Rosenblum, Phys. Lett. **8**, 308 (1964).
- ²⁵ G. Bon Mardin, B. B. Goodman, and A. Lacaze, Phys. Lett. **8**, 15 (1964).
- ²⁶ M. Strongin, A. Paskin, D. G. Schweitzer, O. F. Kammerer, and P. P. Craig, Phys. Rev. Lett. **12**, 442 (1964).
- ²⁷ E. L. Thomas, H. -O. Lee, A. N. Bonkston, S. MaQuilon, P. Klavins, M. Moldovan, D. P. Young, Z. Fisk, and J. Y. Chan, J. Sol. State Chem. **179**, 1642 (2006).
- ²⁸ T. Mishra, Ch. Schwickert, T. Langer, and R. Pöttgen, Z. Naturforsch. b, **66**, 664 (2011).
- ²⁹ A.M. Gabovich, Mai Suan Li, M. Pekała, H. Szymczak, A.I. Voitenko, Physica C **405**, 187 (2004).
- ³⁰ J. L. Olsen, E. Bucher, M. Levy, J. Muller, E. Corenzwit, and T. Geballe, Rev. Mod. Phys. **36**, 168 (1964).
- ³¹ G. M. Eliashberg, Sov. Phys. JEPT **11**, 696 (1960); **12**, 1000 (1961).
- ³² W. L. McMillan, Phys. Rev. **167**, 331 (1967).
- ³³ R. C. Dynes, Sol. State Commun. **10**, 615 (1972).
- ³⁴ Y. Shao and X. Zhang, J. Phys.:Condens. Matter **16**, 1103 (2004).
- ³⁵ I. Martin, D. Podolsky, and S. A. Kivelson, Phys. Rev. B **72**, 060502(R) (2005); M. M. Maška, Ž. Śledz, K. Czajka, and M. Mierzejewski, Phys. Rev. Lett. **99**, 147006 (2007); M. V. Feigelman, L. B. Ioffe, V. E. Kravtsov, and E. A. Yuzbashyan, Phys. Rev. Lett. **98**, 027001 (2007); I. S. Burmistrov, I. V. Gornyi, and A. D. Mirlin, Phys. Rev. Lett. **108**, 017002 (2012).
- ³⁶ V. Z. Kresin, H. Morawitz, and S. A. Wolf, “Superconducting State: Mechanisms and Properties”, (Oxford University Press, Oxford, 2014), Edition I